Electronic Supplementary Material (ESI) for Analytical Methods.
This journal is © The Royal Society of Chemistry 2024

Electronic Supplementary Information

PCB-C^{4}D coupled with paper-based microfluidic sampling for the rapid detection of liquid conductivity

Mingpeng Yang,[*ab] Mingyi Cao,[a] Zhixuan Zhang,[c] Chaofan Wang[a]

[a] School of Automation, Nanjing University of Information Science and Technology, 219 Ningliu Road, Nanjing 210044, China

[b] Jiangsu Collaborative Innovation Centre on Atmospheric Environment and Equipment Technology, Nanjing University of Information Science and Technology, 219 Ningliu Road, Nanjing 210044, China

[c] China Aero Geophysical Survey and Remote Sensing Center for Natural Resources, 29 Xueyuan Road, Beijing 10083, China

1. Principle of signal processing for conductivity measurement

A function signal generator generates an alternating current (AC) sinusoidal excitation signal with a specific frequency, which is applied to the excitation electrode E1. This signal traverses the test liquid and reaches the signal reception electrode E2. It undergoes I/V conversion and amplification through the I/V conversion amplification circuit. The amplified signal is then combined with the reference signal with the same frequency and phase as the excitation signal, generated by the function signal generator. This combination is achieved using a multiplier, resulting in a composite signal comprising a direct current (DC) component and an alternating current (AC) component. To effectively eliminate AC component, a low-pass filter is employed. The resulting output is a DC signal, the amplitude of which correlated with the conductivity of the test liquid.

In this study, two high-frequency alternating current signals, namely the excitation signal and the reference signal, were respectively input. The expression of the excitation signal is assumed as:

$$\mathrm{e}(t) = V_0 \cos(\omega_0 t + \theta) \tag{1}$$

The expression of the input reference signal is:

$$r(t) = V_1 \cos(\omega_0 t) \tag{2}$$

Here, V_0 represents the amplitude of the excitation signal, V_1 represents the amplitude of the reference signal, ω_0 represents the frequency of the excitation signal and the reference signal, and θ represents the phase difference between the two signals.

When the two signals are processed by the multiplier, the output of the multiplier module can be obtained as:

$$\begin{aligned} u_p(t) &= \mathrm{e}(t) * r(t) \\ &= V_0 \cos(\omega_0 t + \theta) * V_1 \cos(\omega_0 t) \\ &= \frac{1}{2} V_0 V_1 \cos\theta + \frac{1}{2} V_0 V_1 \cos(2\omega_0 t + \theta) \end{aligned} \tag{3}$$

It is noted from equation (3) that the output of the multiplier is a composite signal consisting of a direct current (DC) component and an alternating current (AC) component. Subsequently, this composite signal passes through a low-pass filtering module to remove high-frequency signals, ultimately yielding a direct current (DC) signal, expressed as:

$$u_0 = \frac{1}{2} V_0 V_1 \cos\theta \tag{4}$$

The amplitude of this direct current signal is related to the conductivity of the tested liquid. When the phase difference between the two input signals $\theta = 0$ (i.e., when the two input signals have the same frequency and phase), $\cos\theta = 1$, and the direct current signal u_0 reaches its maximum value. Therefore, we pre-adjusted the frequencies and phases of the excitation signal and the reference signal to be the same using a dual-channel oscilloscope to obtain the maximum output voltage of the signal before starting the experiment.

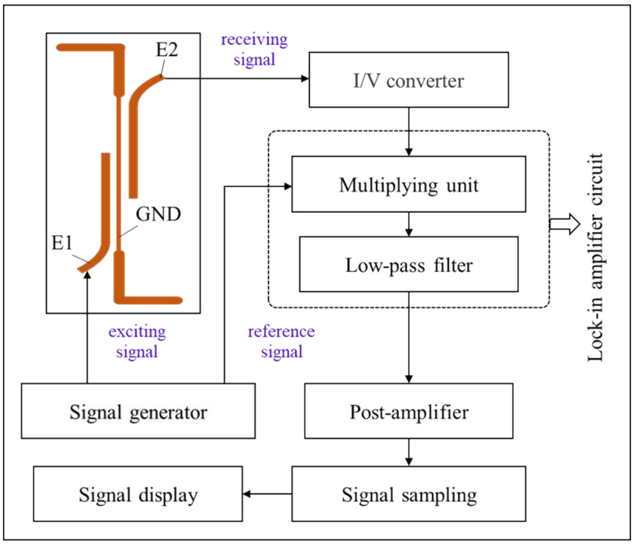

Fig. S1 Schematic diagram of the C[4]D signal processing circuit.

2. Data acquisition and microcontroller unit (MCU) workflow diagram for signal analysis

This analog DC signal undergoes analog-to-digital conversion (ADC) before being transmitted to a microcontroller unit (MCU). Specifically, a high-precision ADC chip, MAX194, was utilized. It is a 14-bit serial successive approximation type analog-to-digital converter. Compared to the built-in 12-bit ADC in the MCU, it offers advantages such as high speed, high precision, and low power consumption. Subsequently, the data is sent to the computer via serial communication for display and analysis.

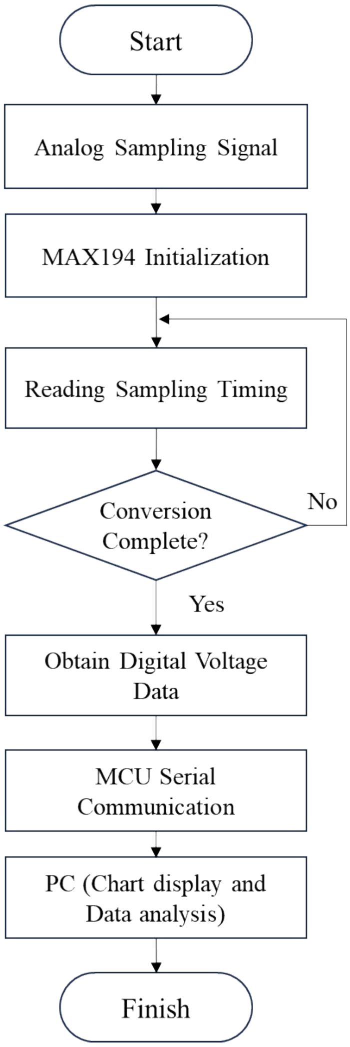

Fig. S2 Workflow diagram of data acquisition and transmission.

3. Detailed circuit schematic for signal processing

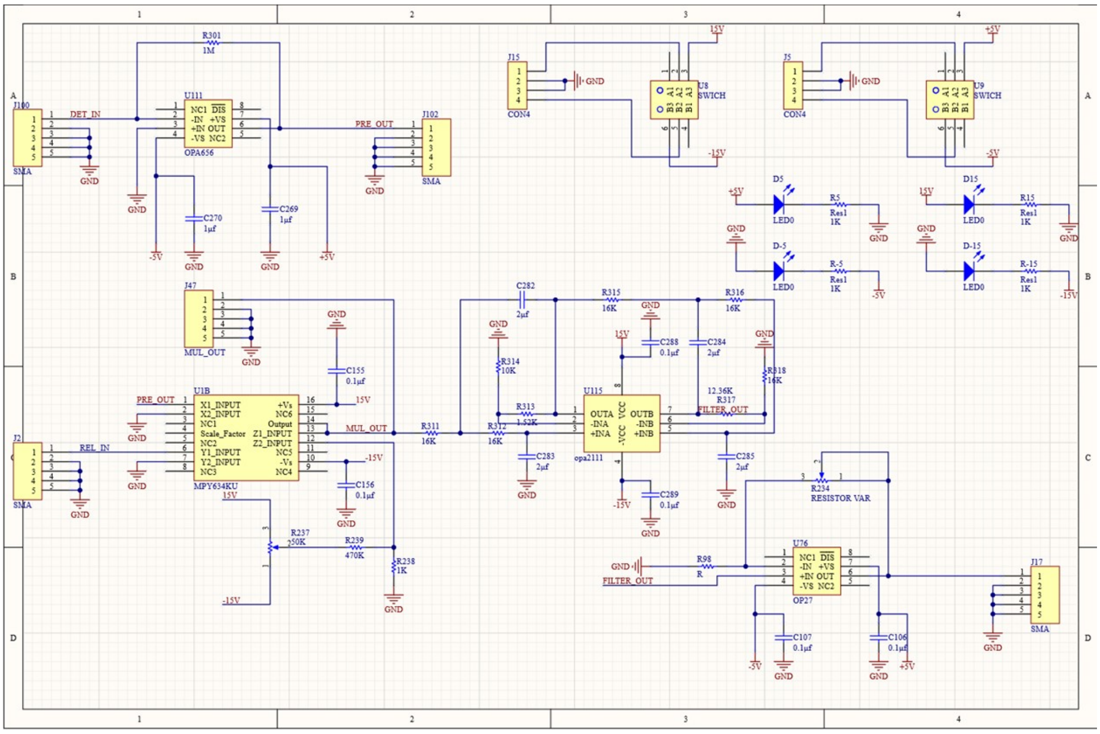

Fig. S3 Detailed Circuit Schematic for Signal Processing.

4. Photographs of the signal processing circuit

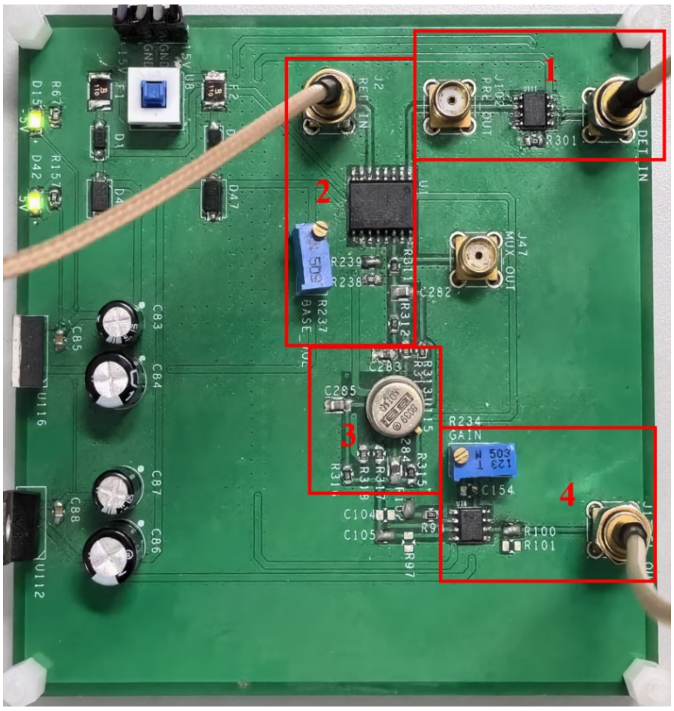

Fig. S4 Photographs of the signal processing circuit 1- I/V conversion; 2- Multiplier; 3- Low-pass filter; 4- Post-amplifier.

5. Experimental platform for the conductivity measurement of liquid samples

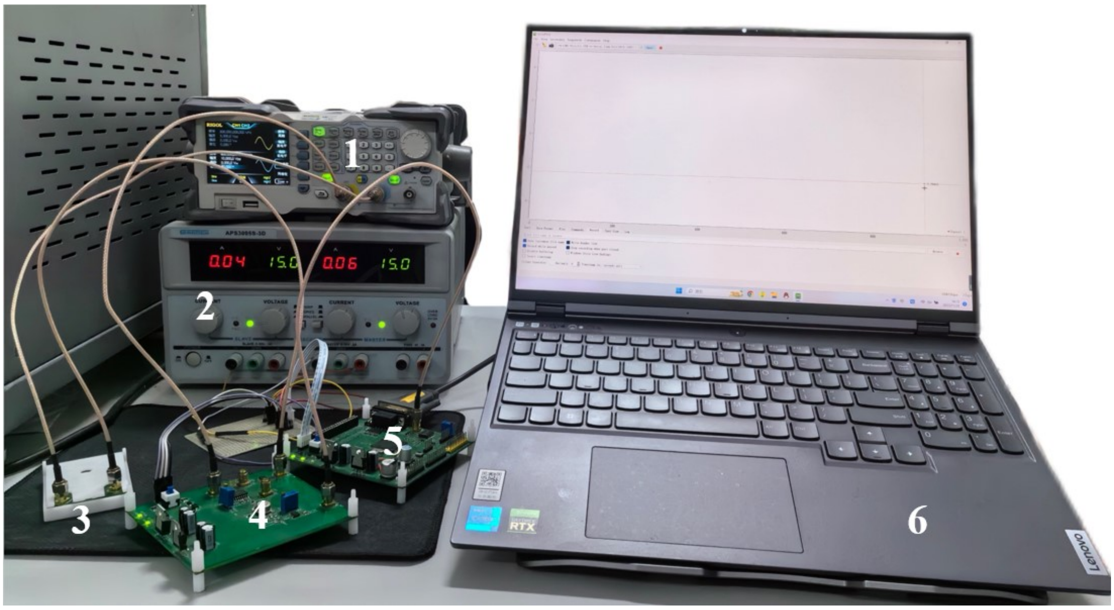

Fig. S5 Experimental platform for the conductivity measurement of liquid samples. 1- Signal generator; 2- Voltage-stabilized source; 3- Paper-based microfluidic detection device; 4- Signal processing circuit; 5- Signal sampling circuit; 6- Computer.

6. Detailed parameters of the slow-speed filter paper used in C^4D signal frequency analysis

Table S1 Detailed parameters of the slow-speed filter paper.

Characteristics of the slow-speed filter paper	
Parameter	Value
Pore size (μm)	3
Material	Cellulose
Nominal ash content (＜%)	0.15
Nominal basis weight (g m^{-2})	80±4
Nominal thickness (μm)	200
Nominal filtration time (s)[a]	110
Wet strength (＞mm water column)[b]	180

[a] Nominal filtration time - Time taken to filter 100mL of distilled water using a $10cm^2$ area filter paper. [b] Wet strength - Determined using a Hercules tester.

7. Solution capacity test of the microfluidic channel

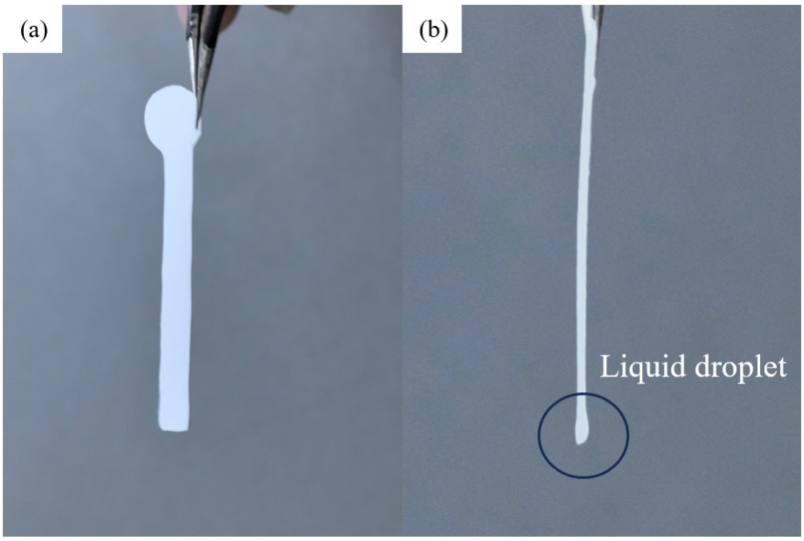

Fig S6 Solution capacity test of the microfluidic channel. (a) Before the experiment starts; (b) Liquid droplet formed at the end of the microfluidic channel filter paper.

8. Equivalent circuit model of the C⁴D device

We investigated the equivalent circuit model of the paper-based microfluidic C⁴D device, as shown in Fig. S8a, where R_s represents the solution resistance, C_s, C_d, and C_i represent the solution capacitance, the double capacitance formed between the insulation layer and the solution surface, and the insulation layer capacitance, respectively, and C_0 represents the parasitic capacitance. Therefore, the total impedance Z_m between the two electrodes can be expressed as:

$$Z_m = (2Z_{C_i} + 2Z_{C_d} + R_s // Z_{C_s}) // 2Z_{C_0} \tag{5}$$

It is known from the paper, "Huck C, Poghossian A, Bäcker M, et al. Capacitively coupled electrolyte-conductivity sensor based on high-k material of barium strontium titanate[J]. Sensors and Actuators B: Chemical, 2014, 198: 102-109.", that C_s is very small and can be neglected. When the excitation signal frequency is low, due to the presence of the grounding electrode between the detection electrodes, Z_{C_0} becomes very large, so the impedance is mainly affected by the series combination of C_d and C_i. At this time, Z_m can be expressed as:

$$Z_m = 2Z_{C_i} + 2Z_{C_d} + R_s \tag{6}$$

As the frequency increases, both Z_{C_i} and Z_{C_d} decrease, causing Z_m to gradually approach R_s.

Nevertheless, with further frequency increase, the equivalent circuit model transforms, as depicted in Fig. S8b. The impact of the parasitic capacitance C_p in the detection circuit on the total impedance Z_m cannot be disregarded. Consequently, Z_m can be expressed as:

$$Z_m = \frac{R_s}{1 + R_s / Z_{C_p}} \tag{6}$$

Based on the above analysis, it is evident that the output value of the C^4D signal can reach its maximum only within a specific frequency band. From the experimental results mentioned above, it can be concluded that 800 kHz is the maximum frequency obtained in our experiment.

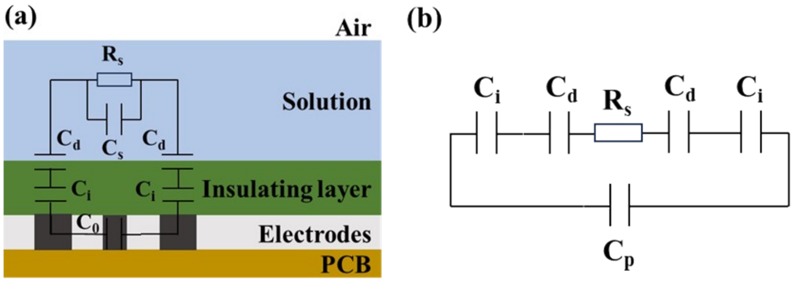

Fig S7 Equivalent circuit model of the C^4D device. (a) Low-frequency C^4D sensor equivalent circuit model. (b) High-frequency C^4D sensor equivalent circuit model.

9. Two linear calibration ranges of the paper-based microfluidic device

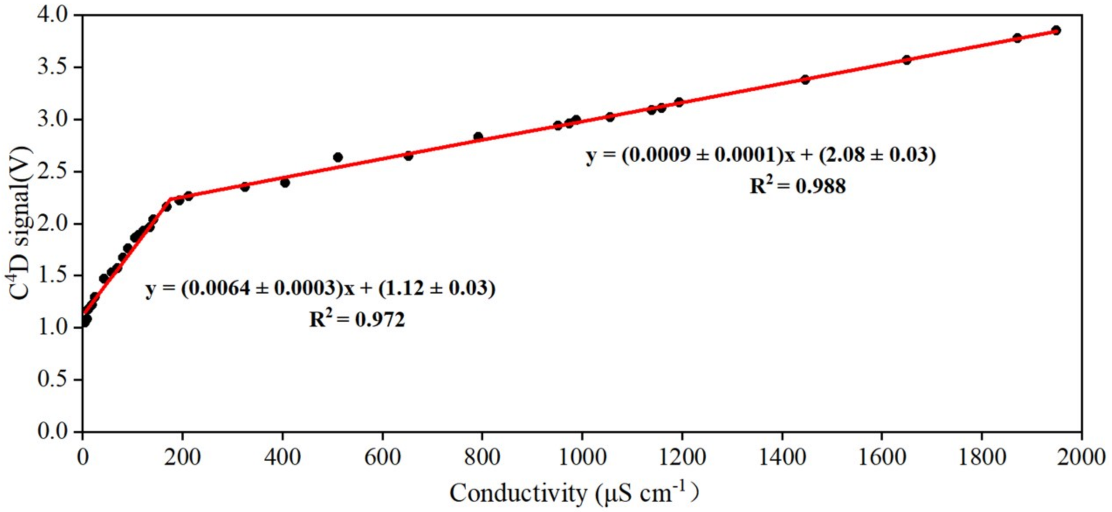

Fig S8 Example of the two linear calibration ranges of the paper-based microfluidic device obtained from dispensing a series of NaCl standard solutions on the paper strip to give a range of conductivity values.

10. Main analytical parameters of repetitive testing results for the electrical conductivity of real solution

Table S2 Main analytical parameters of repetitive testing (n=3) results for the electrical conductivity of orange juice solution.

Channel type	Channel size (mm × mm)	Pre-processed[a]	Mean of C^4D signal (V) (n=3)	RSD (%)	Detection Time (s)
Channel 1	4 × 10	Yes	2.76	0.068	2.9
Channel 2	4 × 10	No	2.24	12.072	3.1
Channel 3	4 × 35	Yes	2.74	0.007	12.2
Channel 4	4 × 35	No	2.76	0.029	12.5

[a] This indicates that prior to measurement, the samples were subjected to both centrifugation and filtration processes. These preparatory steps ensure the removal of particulates.

Table S3 Main analytical parameters of repetitive testing (n=3) results for the electrical conductivity of cucumber solution.

Channel type	Channel size (mm × mm)	Pre-processed[a]	Mean of C^4D signal (V) (n=3)	RSD (%)	Detection Time (s)
Channel 1	4 × 10	Yes	1.98	0.041	2.8
Channel 2	4 × 10	No	1.41	16.466	2.9
Channel 3	4 × 35	Yes	1.98	0.031	12.1
Channel 4	4 × 35	No	1.97	0.021	11.8

[a] This indicates that prior to measurement, the samples were subjected to both centrifugation and filtration processes. These preparatory steps ensure the removal of particulates.

Table S4 Main analytical parameters of repetitive testing (n=3) results for the electrical conductivity of soil suspension.

Channel type	Channel size (mm × mm)	Pre-processed[a]	Mean of C^4D signal (V) (n=3)	RSD (%)	Detection Time (s)
Channel 1	4 × 10	Yes	2.57	0.058	2.7
Channel 2	4 × 10	No	1.96	11.465	2.8
Channel 3	4 × 35	Yes	2.57	0.042	12.2
Channel 4	4 × 35	No	2.56	0.024	12.4

[a] This indicates that prior to measurement, the samples were subjected to both centrifugation and

filtration processes. These preparatory steps ensure the removal of particulates.